

Connection between memory performance and optical absorption in quantum reservoir computing

Niclas Götting,¹ Steffen Wilksen,¹ Alexander Steinhoff,² Frederik Lohof,² and Christopher Gies¹

¹*Institute for Physics, Faculty V, Carl von Ossietzky University Oldenburg, 26129 Oldenburg, Germany*

²*Institute for Theoretical Physics, University of Bremen, 28359 Bremen, Germany*

(Dated: January 28, 2025)

The fading memory property is a key requirement for reservoir computers – a specific type of recurrent neural network with fixed internal weights. While mostly undesired in gate-based quantum computing, dissipation due to material imperfections or coupling to the environment acts as a natural mechanism intrinsically providing fading memory to reservoir computers based on dynamical open quantum systems. In this work, we unravel a connection between the physical metric of optical absorption and the performance of quantum reservoir computers in terms of their short-term memory capacity. We establish this link by considering a coherent input encoding in conjunction with tunable qubit decay, giving precise control over the fading memory in the quantum reservoir computer. Our analysis enables us to identify a sweet-spot regime for the dissipation strength at which memory performance is maximized.

INTRODUCTION

Reservoir computers are a specific implementation of recurrent neural networks (RNNs) [1, 2]. While both rely on backward connections to achieve a computational memory intrinsic to the network, reservoir computing (RC) eliminates the excessive cost of training the RNN by assigning fixed, random weights and only training a linear readout layer [3, 4]. The weights being fixed enables realization of the RC framework on non-programmable physical hardware, which opens up a wide variety of platforms for physical RC, reaching from origami structures [5] to all-optical setups [6].

In recent years, quantum systems emerged as an intriguing new RC platform, due to their unique properties such as the – with respect to system size – exponentially scaling phase space, superposition, entanglement, and the ability to process native quantum data [7–9]. Like their classical counterparts, quantum reservoir computers acting on bi-infinite time series data [10] rely on the so-called *fading memory property* [11] to not depend on inputs arbitrarily far in the past. Initial concepts of quantum reservoir computing (QRC) models utilized a projective erase-and-write map for input encoding to introduce dissipation to otherwise ideal quantum systems as a means to fade out past information [8, 12–14]. While this approach provides a theoretically feasible scheme for QRC, it suffers from performance losses in the presence of additional dissipation due to imperfections in more realistic, noisy intermediate-scale quantum (NISQ) reservoir computers based on open quantum systems. To address this problem, newer models use unitary input encodings on top of a quantum system with tunable dissipation, resulting not only in an operationally more robust setup, but also a new parameter to optimize the model’s performance [15–18].

In this work, we connect the performance of such a coherently driven QRC setup with tunable dissipation in terms of its short-term memory capacity (STMC) to its optical absorption. We expect the absorption to have a

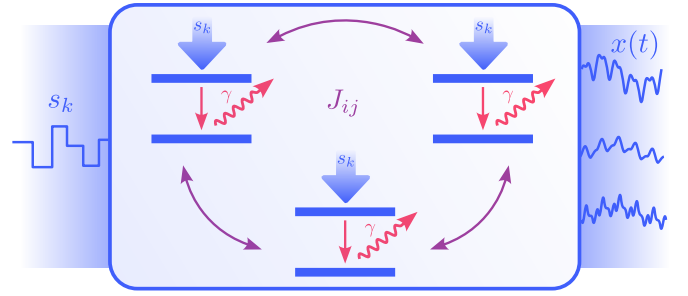


FIG. 1. Schematic representation of the coupling matrix elements J_{ij} , the qubit decay γ , and the input injection pump of strength s_k , with the qubit decay and the pump strength being equal for all qubits. For the 3-qubit case depicted here, we receive a 3-dimensional output function $x(t)$.

strong impact on the reservoir’s computational performance, as it is the channel over which the information – encoded in a coherent light source – is injected into the reservoir. By calculating the absorption over a large range of possible dissipation strengths, we find a sweet spot regime that directly correlates with the STMC of the quantum reservoir computer. This facilitates engineering of quantum hardware specifically for memory intensive QRC applications.

DISSIPATIVE QUANTUM SYSTEMS FOR QRC

To investigate the effects of dissipation in QRC, we use the fully-connected transverse-field Ising model (TFIM) [19]

$$H = \sum_{i < j} J_{ij} \sigma_x^{(i)} \sigma_x^{(j)} + h \sum_i \sigma_z^{(i)} \quad (1)$$

as the physical platform for computation, because it incorporates enough complexity to simulate non-trivial qubit networks while still being computationally accessible. The qubit energy h is typically set to 1, while

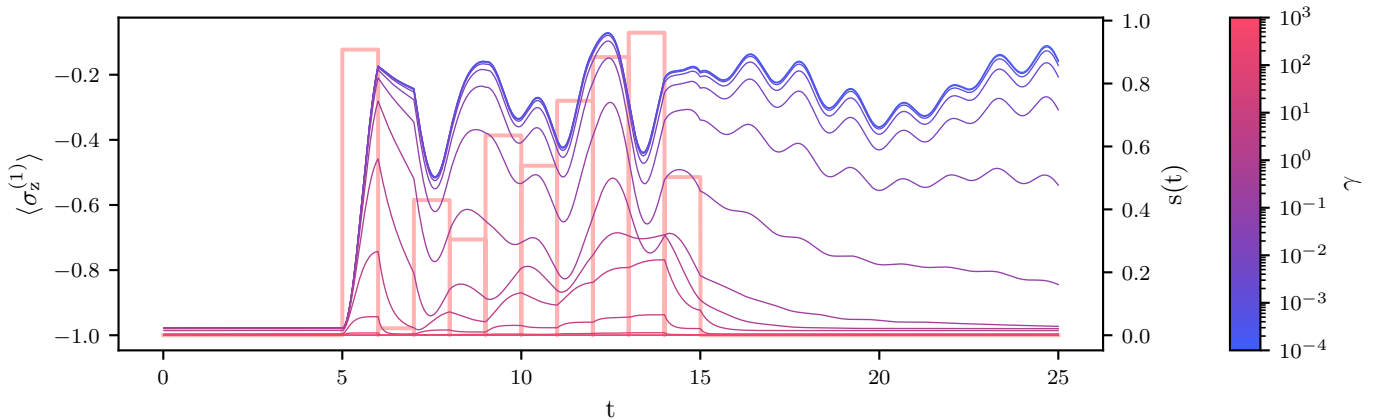


FIG. 2. Time evolution of the σ_z expectation value of the first qubit in a 3-qubit TFIM for different qubit decay strengths γ . In light red (right axis) the input signal is displayed.

the coupling matrix J_{ij} is chosen randomly and then scaled to a certain spectral radius J_0 , which we refer to as the *coupling strength*. The expectation values of the σ_z observable of each qubit form the reservoir computer's N -dimensional readout function $x(t)$, where N is the number of qubits in the system. We sample the readout function at each timestep k and subsample V -times between inputs to implement a time multiplexing. In addition to these signals, a bias term of 1 is added to the readout, resulting in the full *state collect matrix* $\mathbf{X} \in \mathbb{R}^{k \times NV+1}$ that includes all recorded expectation values and the bias. The output vector \mathbf{y} is then constructed from the state collect matrix by applying a linear weight vector \mathbf{w} that minimizes the L^2 distance to the target vector $\hat{\mathbf{y}}$, i.e. $\mathbf{w} = \arg \min_{\mathbf{w}} |\hat{\mathbf{y}} - \mathbf{w}\mathbf{X}|^2$.

In many previous approaches [8, 12, 13], the computational input is injected into the system via an erase-and-write map $\rho \mapsto \rho_{\text{in}}(s_k) \otimes \text{Tr}_1 \rho$, which resets a designated input qubit to a new state parametrized by the input value s_k . The drawback of this type of input encoding is that it introduces a fixed amount of dissipation to the process, which acts on top of the natural dissipation of the NISQ hardware, reducing the possibilities for dissipation engineering. We therefore choose instead as the input medium a coherent light source, which couples resonantly to the qubits in the TFIM and is amplitude modulated according to the input signal, inducing no inherent dissipation; this allows for complete control over the dissipation strength in the simulation. To avoid the computationally costly explicit modelling of the light field, an effective σ_y -term is added to the dynamics emulating the coherent input encoding. In the rotating frame of the pump, which we use to eliminate the impact of the qubit energy σ_z at resonant excitation from the calculation, we obtain the time-dependent Hamiltonian

$$H(t) = \sum_{i < j} J_{ij} \sigma_x^{(i)} \sigma_x^{(j)} + s(t) \sum_i \sigma_y^{(i)} \quad (2)$$

with $s(t) = s_{\lfloor t \rfloor}$.

As this setup so far features only unitary dynamics, it does not exhibit a fading memory and can thus not be used as a reservoir computer. However, real NISQ systems are subject to various types of dissipation that force the time evolution into a steady state, which – when unique – is independent of the initial state, making the system suitable for RC.

To make the analysis more concise, we restrict ourselves to one specific type of dissipation in the simulation, namely the qubit decay. We model its impact on the TFIM time evolution with the Gorini–Kossakowski–Sudarshan–Lindblad (GKSL) equation [20], consisting of the unitary von-Neumann dynamics and a dissipative part that here describes the qubit decay. The full dynamics of the density operator is then given by

$$\dot{\rho} = -i[H(t), \rho] + \sum_i \gamma_i \left(\sigma_-^{(i)} \rho \sigma_+^{(i)} - \frac{1}{2} \left\{ \sigma_+^{(i)} \sigma_-^{(i)}, \rho \right\} \right), \quad (3)$$

where $\gamma_i \equiv \gamma$ is the decay rate of the qubits, and $\sigma_-^{(i)}$ ($\sigma_+^{(i)}$) is the lowering (raising) operator of qubit i . Because the reservoir dissipation is naturally occurring and not solely when a new input is injected, it is not required to introduce a washout sequence into the process for common-signal-induced synchronization (CSIS) [21]. Instead, the dissipative quantum reservoir computer assumes a known steady state to arbitrary precision after a certain amount of waiting time. To calculate this steady state, we first reformulate Eq. (3) to Fock-Liouville space (FLS), yielding a Liouvillian superoperator \mathcal{L} , such that

$$\dot{\rho} = \mathcal{L}\rho. \quad (4)$$

In this new representation, the complex mathematical structure of Eq. (3) turns into a linear, ordinary differential equation, which can be solved for the steady-state condition $\mathcal{L}\rho_{\text{ss}} = 0$.

We showcase an exemplary time evolution of a 3-qubit dissipative quantum reservoir computer in Fig. 2, where

the σ_z expectation value of the first qubit is displayed for varying qubit decays and a coupling strength of 0.5. To test the steady-state behavior, we leave the excitation Hamiltonian off for the first five steps and indeed obtain a constant time evolution, indicating that the correct steady-state solution was found. We follow the zero-input stage by ten randomly chosen inputs and then turn the signal off again for ten steps, to give an idea about the “free” time evolution of the TFIM.

Upon injection of the first nonzero input signal, the system is driven out of its steady state to a varying extent, depending on the qubit decay. For very large decays, the deviation from the zero-input steady state is negligible, especially when noise is added to the simulation. In cases where the decay itself becomes negligible compared to the timescales of the model, the unitary dynamics dominate and we observe strong oscillations in the output signal, making the system again unusable for QRC. Already from this analysis it is intuitive that the regime interesting for QRC should be in the range $10^{-1} < \gamma < 10^1$, where the system gets close to a new steady state – which is distinct from the zero-input steady state – during each input injection period, but does not quite reach it. In the next section, we analyze the system to gain a more in-depth understanding on how the qubit decay affects the system performance.

BOUNDS OF DISSIPATION

The key property a physical system needs for RC is the ability to (non-)linearly process past inputs, also called *short-term memory capacity (STMC)* [22]. In its linear form, the corresponding task consists of recovering past inputs $s_{k-\tau}$ from the current output states \mathbf{X}_k . This concept has already been enhanced and extended to more sophisticated measures like the information processing capacity (IPC) [23] or the maximally well reproducible functions of the reservoir – the so-called *eigentasks* [24, 25].

To keep the discussion more concise, we resort here to a reduced form of the IPCs for our analysis, which quantifies the ability of the reservoir computer to reproduce Legendre polynomials of the input sequence up to a certain degree. The quality of the reproduction for each degree i and delay τ is measured by the squared Pearson correlation coefficient

$$C_i^\tau = \frac{\text{cov}^2(\mathbf{y}, \hat{\mathbf{y}}_i)}{\sigma^2(\mathbf{y})\sigma^2(\hat{\mathbf{y}}_i)}, \quad (5)$$

where $\sigma(\cdot)$ is the standard deviation and $\text{cov}(\cdot)$ the covariance. We denote the target sequence $(P_i(s_{k-\tau}), P_i(s_{k-\tau-1}), P_i(s_{k-\tau-2}), \dots)$ as $\hat{\mathbf{y}}_i$, where $P_i(\cdot)$ is the i -th Legendre polynomial rescaled to the interval $[0, 1]$. The length of the training and testing sequences are both fixed to 1000 steps. As our RC system exhibits a dynamically fading memory, the capacities C_i^τ need to

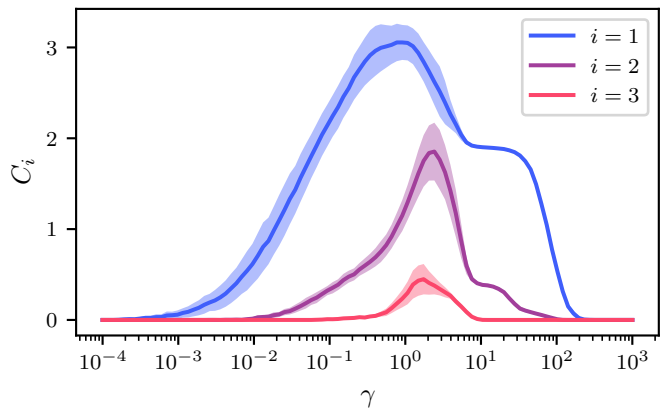


FIG. 3. First three degrees of the STMC of 15 randomly sampled 3-qubit systems for different qubit decays.

vanish for large τ , allowing us to sum up the STMCs for all delays up to a certain τ_{\max} to define a *total memory capacity* $C_i := \sum_{\tau=0}^{\tau_{\max}} C_i^\tau$ for each degree i .

Finding sensible values for τ_{\max} is not a trivial task, as the correlation between two random functions is nonzero in general, resulting in a noise tail of the capacities C_i^τ , even for very large τ . To quantify this noise floor, we correlate the reservoir output \mathbf{y} with a random target function, such that the thereby obtained capacities do not represent an actual memory effect, but rather random correlations. We note that these correlations depend only on the trained weights and network architecture, not the delay τ . The process of calculating these “noise capacities” is repeated 500 times and we take the largest resulting capacity to define the *noise threshold* C_i^{thresh} for each degree i . Once a value in the sequence (C_i^τ) drops below this noise threshold we cut the sequence at that τ and receive the maximum delay τ_{\max} .

With the framework set, we now calculate the total memory capacities of degrees 1, 2, and 3 for varying strengths of the qubit decay as shown in Fig. 3. For small decays, where the system evolves approximately unitarily, the quantum reservoir computer is not able to recall any of the past inputs, so that $C_i^\tau \equiv 0$. Interestingly, the linear STMC displays a strong increase at around $\gamma \gtrsim 10^{-2}$, with the higher order degrees following shortly after. Indeed, as proposed in the last section, we then find a regime of optimal memory capacity for intermediate qubit decays, until again the capacities drop to zero for $\gamma \gtrsim 10^2$. As higher degrees follow a similar trend, but exhibit lower capacities overall in this setup, we will restrain the following discussion to the linear STMC. We also note that the data provided was obtained by simulating shot noise corresponding to 10^6 shots; for the infinite shot ideal case, see the Supplementary Material.

While we gave a general intuition for the behavior of the STMC in Fig. 2, there is typically not much insight obtained about the underlying processes purely from numerical simulations of the reservoir dynamics. By virtue of the reservoir computer being an open quantum system

with a modulated light field as the input injection mechanism, we can, however, facilitate an understanding of the sweet-spot behavior via the analysis of actual physical properties of the qubit network. In this work we propose the absorption α of the qubit system as the main property driving its capability to remember. According to linear response theory the frequency-dependent absorption of a network of two-level systems is given by the normalized dipole correlation's Fourier spectrum [26, 27]

$$\begin{aligned}\alpha_{s,\gamma}(\omega) &= \text{Re} \int_0^\infty e^{-i\omega t} \frac{\text{Tr}[\Sigma_x \Sigma_x(t) \rho_{ss}]}{\text{Tr}[\Sigma_x^2 \rho_{ss}]} dt \\ &= \text{Re} \int_0^\infty e^{-i\omega t} \frac{\text{Tr}[\Sigma_x e^{\mathcal{L}[s,\gamma]t} \Sigma_x \rho_{ss}]}{\text{Tr}[\Sigma_x^2 \rho_{ss}]} dt,\end{aligned}\quad (6)$$

where $\Sigma_x = \sum_i \sigma_x^{(i)}$ is the total dipole moment operator. Here, the additional dependence of the absorption on the signal strength s is explicitly marked, as the external field strongly influences the Hamiltonian structure and thus the absorption spectrum. This circumstance requires the calculation of absorption spectra over the whole range of signal strengths, which are then averaged to get a mean response of the TFIM to optical excitation. We justify this decision by the fact that the 1000 testing input signals are uniformly chosen, such that no specific signal strength has a prominent effect on the resulting STMCs, but rather the average ensemble of signals.

In order for the integral in Eq. (6) to converge, the trace term needs to vanish for large t , which is, however, prevented by the external pumping that results in a constant tail of the correlation function. This effect was attributed by Mollow to elastic scattering of the pump light in [28] and leads to a delta peak in the absorption spectrum at the pump frequency. As the delta peak is only an artifact of the monochromatic light source, we remove it by subtracting the value of the constant tail of the correlation function and obtain a meaningful absorption spectrum as can be seen in Fig. 5 in the Supplementary Material for $s = 1$ and different qubit decays.

In the following discussion we will only investigate the resonant absorption $\alpha_{s,\gamma}(0)$, which corresponds to the qubit system's absorption at the pump frequency and is shown for 10 different values of s and varying qubit decays in Fig. 4 as the light colored curves. It becomes evident that the signal strength – which was discussed before to have a considerable influence on the absorption spectrum – in fact shifts the absorption peak by several orders of magnitude in the qubit decay. This effect appears to be most prominent for smaller signal strengths up to about 0.5, after which the σ_y -term in the Hamiltonian becomes dominant and increasing it does not change the dynamics structurally. Note, that we chose a coupling strength of 0.5 for these results. The behavior of the absorption spectrum hints at the possibility to tune either the qubit decays individually, the qubit couplings or the signal strength range to maximize the absorption, which we leave for future work. As explained above, we average

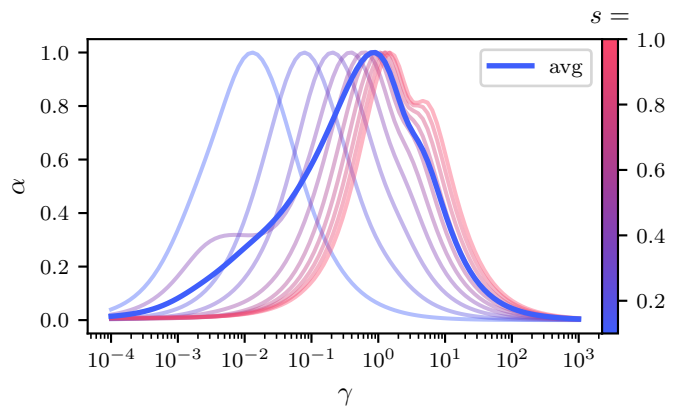


FIG. 4. Resonant absorption $\alpha_{s,\gamma}(0)$ of the same 15 randomly sampled 3-qubit system as in Fig. 3 for different signal strengths s and qubit decays γ . The thick blue line marks the average over all light curves.

over all signal strengths to receive an average absorption $\bar{\alpha}_\gamma$ resembling the mean response of the TFIM to excitation. In Fig. 4, this average response is illustrated by the thick blue line and, remarkably, shows a qualitatively very similar behavior as the STMC in Fig. 3: We find a slow rising edge starting from around $\gamma = 10^{-3}$, developing to a maximum at a decay of approximately 1 and then decreasing again a lot faster to vanish completely at roughly $\gamma = 10^2$. The similarities between STMC and absorption at the extremes of very strong and close to vanishing qubit decay, respectively, follow the intuition that the system cannot possibly remember any information if it is not able to absorb it in the first place. From the data between the extremes, and especially in the sweet spot regime around the peak, we deduce that there exists a significant correlation between the two quantities. The observed behavior aligns with our expectations that the reservoir computer is more effectively supplied with information in the strong absorption regime and should thus also be able to better reproduce it. These results reveal a link between two – at first glance – completely unrelated properties, the first one being the information theoretical STMC and the second one the physical property of the optical absorption.

CONCLUSION

We have demonstrated a connection between the performance of quantum reservoir computers and their optical absorption properties in the presence of a tunable qubit decay. By using a coherent input encoding, the dephasing can be used to precisely tune the fading-memory property of the reservoir, revealing the same distinct behavior of the memory performance and the absorption as function of the dissipation strength. In particular, we find a sweet spot of optimal memory capacity. This insight opens up a new avenue for hardware design in dynamical

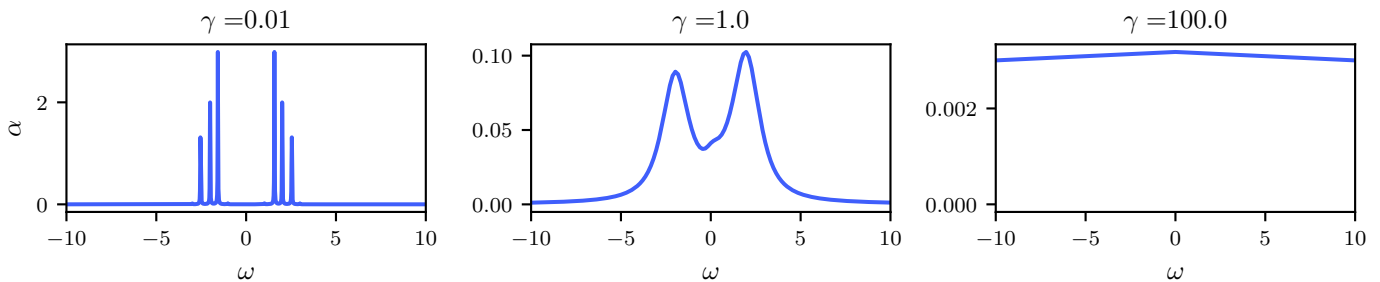


FIG. 5. Absorption spectra for qubit decays $\gamma \in \{10^{-2}, 10^0, 10^2\}$ and an input signal strength of $s = 1$. The zero-frequency components correspond to points on the absorption curve for $s = 1$ in Fig. 4

quantum computing, where performance metrics can be deduced from physical properties directly accessible to optical measurements. Following this pathway, it may become possible in the future to tailor a quantum reservoir computer’s physical properties specifically to given computing task.

Acknowledgements We gratefully acknowledge funding by the Deutsche Forschungsgemeinschaft (German Science Foundation, DFG) via the project PhotonicQRC (Gi1121/6-1).

Absorption spectra

To gain a better insight regarding the structure of the absorption curves in Fig. 4 in the main text, we here show three exemplary absorption spectra for the input strength $s = 1$ and three different qubit decays in Fig. 5. For a small decay ($\gamma = 10^{-2}$), we find sharp peaks centered around the zero-frequency in the absorption spectrum, which are a result of the external pumping and change in position for different input signals. Upon increasing the dissipation strength, the typical line broadening occurs and allows for the absorption of information in the pump frequency of $\omega = 0$ – it is around this dissipation that the absorption, and with it the STMC, is maximized. Elevating the dissipation even further to $\gamma = 100$ leads to an almost completely flat spectrum, as the line broadening washes away all structure in the spectrum.

Infinite shot STMC

As discussed in the main text, Fig. 3 depicts the STMC for finite shot noise corresponding to 10^6 measurements. In the infinite shot case as shown in Fig. 6, however, we observe a slightly different behavior of the STMC for larger decays; even the most minute deviations from the zero-input steady state can be utilized by the noiseless reservoir computer to extract the current input, resulting in a linear STMC of almost exactly one. We find that higher orders of the STMC do not benefit to the same degree from the absence of noise and still drop close to zero for large decays.

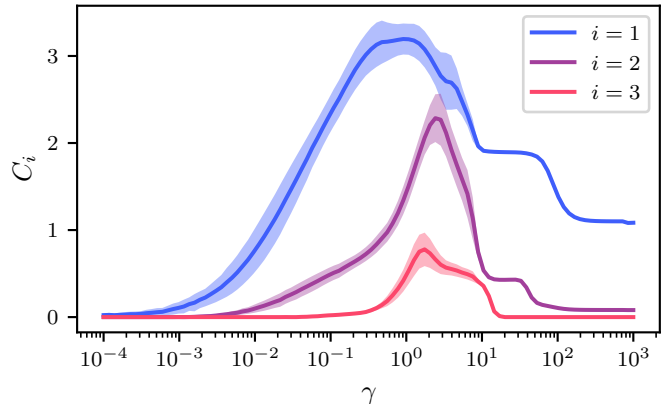


FIG. 6. The first three STMCs for varying qubit decay strength and zero shot noise. As opposed to the results with finite shot noise in Fig. 3, the capacities do not vanish for large qubit decays.

-
- [1] J. L. Elman, Finding Structure in Time, *Cognitive Science* **14**, 179 (1990).
 - [2] M. I. Jordan, *Serial Order: A Parallel Distributed Processing Approach. Technical Report, June 1985-March 1986*, Tech. Rep. AD-A-173989/5/XAB; ICS-8604 (California Univ., San Diego, La Jolla (USA). Inst. for Cognitive Science, 1986).
 - [3] H. Jaeger, The “Echo State” Approach to Analysing and Training Recurrent Neural Networks, GMD-Report 148, German National Research Institute for Computer Science (2001).
 - [4] W. Maass, T. Natschläger, and H. Markram, Real-time computing without stable states: A new framework for neural computation based on perturbations, *Neural Computation* **14**, 2531 (2002).
 - [5] P. Bhowad and S. Li, Physical reservoir computing with origami and its application to robotic crawling, *Scientific Reports* **11**, 13002 (2021).
 - [6] F. Dupont, B. Schneider, A. Smerieri, M. Haelterman, and S. Massar, All-optical reservoir computing, *Optics Express* **20**, 22783 (2012).
 - [7] S. Ghosh, A. Opala, M. Matuszewski, T. Paterek, and T. C. H. Liew, Reconstructing Quantum States With Quantum Reservoir Networks, *IEEE Transactions on Neural Networks and Learning Systems* **32**, 3148 (2021).

- [8] N. Götting, F. Lohof, and C. Gies, Exploring quantumness in quantum reservoir computing, *Physical Review A* **108**, 052427 (2023).
- [9] M. A. Nielsen and I. L. Chuang, *Quantum Computation and Quantum Information*, 10th ed. (Cambridge University Press, Cambridge ; New York, 2010).
- [10] S. Sugiura, R. Ariizumi, T. Asai, and S.-I. Azuma, Nonessentiality of Reservoir’s Fading Memory for Universality of Reservoir Computing, *IEEE Transactions on Neural Networks and Learning Systems* **35**, 16801 (2024).
- [11] T. L. Carroll, Optimizing Memory in Reservoir Computers, *Chaos: An Interdisciplinary Journal of Nonlinear Science* **32**, 023123 (2022), arXiv:2201.01605 [cs].
- [12] K. Fujii and K. Nakajima, Harnessing Disordered-Ensemble Quantum Dynamics for Machine Learning, *Physical Review Applied* **8**, 024030 (2017).
- [13] R. Martínez-Peña, J. Nokkala, G. L. Giorgi, R. Zambrini, and M. C. Soriano, Information Processing Capacity of Spin-Based Quantum Reservoir Computing Systems, *Cognitive Computation* 10.1007/s12559-020-09772-y (2020).
- [14] A. Palacios, R. Martínez-Peña, M. C. Soriano, G. L. Giorgi, and R. Zambrini, Role of coherence in many-body Quantum Reservoir Computing, *Communications Physics* **7**, 1 (2024).
- [15] F. Monzani, E. Ricci, L. Nigro, and E. Prati, Leveraging non-unital noise for gate-based quantum reservoir computing (2024), arXiv:2409.07886 [quant-ph].
- [16] M. L. Olivera-Atencio, L. Lamata, and J. Casado-Pascual, Benefits of Open Quantum Systems for Quantum Machine Learning, *Advanced Quantum Technologies* , 2300247 (2023).
- [17] A. Sanna, R. Martínez-Peña, M. C. Soriano, G. L. Giorgi, and R. Zambrini, Dissipation as a resource for Quantum Reservoir Computing, *Quantum* **8**, 1291 (2024), arXiv:2212.12078 [quant-ph].
- [18] L. Domingo, G. Carlo, and F. Borondo, Taking advantage of noise in quantum reservoir computing, *Scientific Reports* **13**, 8790 (2023).
- [19] P. Pfeuty and R. J. Elliott, The Ising model with a transverse field. II. Ground state properties, *Journal of Physics C: Solid State Physics* **4**, 2370 (1971).
- [20] D. Manzano, A short introduction to the Lindblad master equation, *AIP Advances* **10**, 025106 (2020).
- [21] M. Inubushi, K. Yoshimura, Y. Ikeda, and Y. Nagasawa, On the Characteristics and Structures of Dynamical Systems Suitable for Reservoir Computing, in *Reservoir Computing: Theory, Physical Implementations, and Applications*, edited by K. Nakajima and I. Fischer (Springer, Singapore, 2021) pp. 97–116.
- [22] H. Jaeger, *Short Term Memory in Echo State Networks* (GMD Forschungszentrum Informationstechnik, 2001).
- [23] J. Dambre, D. Verstraeten, B. Schrauwen, and S. Massar, Information Processing Capacity of Dynamical Systems, *Scientific Reports* **2**, 514 (2012).
- [24] F. Hu, G. Angelatos, S. A. Khan, M. Vives, E. Türeci, L. Bello, G. E. Rowlands, G. J. Ribeill, and H. E. Türeci, Tackling Sampling Noise in Physical Systems for Machine Learning Applications: Fundamental Limits and Eigentasks, *Physical Review X* **13**, 041020 (2023).
- [25] A. M. Polloreno, Limits to Reservoir Learning (2023), arXiv:2307.14474 [cs, math].
- [26] T.-M. Chang and J. Skinner, Non-Markovian population and phase relaxation and absorption lineshape for a two-level system strongly coupled to a harmonic quantum bath, *Physica A: Statistical Mechanics and its Applications* **193**, 483 (1993).
- [27] D. A. McQuarrie, *Statistical Mechanics* (2000).
- [28] B. R. Mollow, Power Spectrum of Light Scattered by Two-Level Systems, *Physical Review* **188**, 1969 (1969).